UC Davis

UC Davis Previously Published Works

Title

Proteomic manifestations of genetic defects in autosomal recessive congenital ichthyosis

Permalink

https://escholarship.org/uc/item/4nz9412g

Authors

Karim, Noreen

Durbin-Johnson, Blythe

Rocke, David M

et al.

Publication Date

2019-06-01

DOI

10.1016/j.jprot.2019.04.007

Peer reviewed

eScholarship.org Powered by the California Digital Library
University of California

Proteomic manifestations of genetic defects in autosomal recessive congenital ichthyosis

Short title: Altered protein profiles in ichthyosis

Noreen Karim[1,2], Blythe Durbin-Johnson[3], David M. Rocke[3], Michelle Salemi[4], Brett S. Phinney[4], Muhammad Naeem[1], Robert H. Rice[2]

[1]Medical Genetics Research Laboratory, Department of Biotechnology, Quaid-i-Azam University, Islamabad, Pakistan

[2]Department of Environmental Toxicology, University of California, Davis, CA

[3]Division of Biostatistics, Department of Public Health Sciences, Clinical and Translational Science Center Biostatistics Core, University of California, Davis, CA

[4]Proteomics Core Facility, University of California, Davis, CA

Correspondence: Dr. Robert H. Rice, Department of Environmental Toxicology, University of California, Davis, CA 95616-8588; Tel 530-752-5176, Fax 530-752-3394, Email rhrice@ucdavis.edu

Acknowledgments

We thank the International Research Support Initiative Program of the Higher Education Commission of Pakistan, the National Center for Advancing Translational Sciences (NIH grant UL1 TR001860) and the USDA(NIFA)/University of California Agricultural Experiment Station for financial support of this work. Sources of funding had no role in study design; in data collection, analysis and interpretation; in writing the report; and in the decision to submit the article for publication.

Proteomic manifestations of genetic defects in autosomal recessive congenital ichthyosis

Abstract

Numerous genetic conditions give rise to a scaly skin phenotype as a result of impaired barrier function. Present work investigates the degree to which the departure from normal of ichthyosis corneocytes on the skin surface depends upon the basic defect as judged by proteomic profiling. Analyzing autosomal recessive congenital ichthyosis arising from defects in the genes *PNPLA1*, *SDR9C7* and *TGM1* revealed that profiles of PNPLA1 samples displayed the greatest degree of departure from normal control epidermis, with SDR9C7 samples nearly as divergent, and TGM1 the least divergent. Although the profiles were distinctive, each displaying a set of altered protein levels, they exhibited alterations in 20 proteins in common, of which 15 were expressed consistently at higher and 5 at lower levels. Departure from the normal profile was examined at three different anatomic sites (forearm, forehead, leg). Reflecting that the normal protein profile differed at these sites, comparing profiles from afflicted subjects revealed that the degree of alteration in profile was site-dependent. These results suggest proteomic profiling can provide a quantitative measure of departure from the normal state of epidermis. Further development may help characterize consequences of the genetic defects, including perturbation of signaling pathways, and supplement visual evaluation of treatment.

Significance

ARCI are rare cornification disorders caused by mutations in at least 14 different genes leading to perturbed metabolism and organization of constituent biomolecules of cornified envelope. The phenotypic manifestations of the disorder vary among individuals with the same as well as

different genetic defect and even at different anatomic sites within the same individual. The present study investigates the proteomic disturbances at three anatomic sites in patients carrying mutations in three different genes. Our findings provide a basis for elucidating genotype to proteome relationships for ARCI, further investigation of which may help to delineate the underlying pathways as well as to identify new drug targets.

1. Introduction

Autosomal Recessive Congenital Ichthyosis (ARCI) comprises a group of rare inherited keratinization disorders characterized by generalized hyperkeratotic epidermal scales, sometimes accompanied by erythroderma. ARCI is categorized in three broad classes based on the phenotypic manifestations: Harlequin Ichthyosis (HI), Lamellar Ichthyosis (LI) and Congenital Ichthyosiform Erythroderma (CIE), HI being the most severe form followed by LI and CIE [1]. Subclasses of the disorder have been reported based on the underlying defects in 14 genes (https://www.omim.org/). These genes are *TGM1, ALOXE3, ALOX12B, ABCA12, NIPAL4, CYP4F22, PNPLA1, CERS3, LIPN, SDR9C7, SLC27A4, ST14, SULT2B1* and *CASP14*, most of which perturb lipid metabolism or localization during cornification, thereby disrupting the lipid envelope and thus barrier function [2,3]. The consequent increases in permeability and transepidermal water loss result in hyperkeratosis, a homeostatic response to the compromised cornified layer to reestablish an intact and competent cutaneous barrier. Severity of the phenotype is directly related to severity of the barrier defect [4].

HI, caused by gross deletions in *ABCA12*, can be readily recognized by the characteristic thick large plate-like scales with deep fissures accompanying severe eclabium, ectropion and flattened ears. However, a spectrum of phenotypes lies between the relatively severe LI and milder CIE types of ARCI. Phenotypes resulting from different causal gene defects differ from each other in

appearance of the scales, collodion membranes, presence or absence of erythroderma, the areas of skin affected and severity of ectropion, eclabium and hypohidrosis. Nevertheless, diagnosis based solely on clinical presentation is difficult [5].

Research is in progress to reduce or treat the disease manifestations in affected individuals, including by lipid replacement, enzyme replacement and gene therapy. To discover more effective drug/treatment targets, gene expression studies in knockout keratinocyte models [6] and histopathological studies of the affected epidermis [7] have been performed. A more precise genotype to phenotype correlation and a greater understanding of the pathophysiology would aid in developing more specific therapies. For this purpose, elucidating the link between a defective gene and the resulting difference in protein levels in epidermis is needed.

Previously, non-invasive protein profiling of ichthyotic epidermal samples in comparison to control has demonstrated differences in protein expression between LI and ichthyosis vulgaris [8]. On that foundation, protein profiles generated from epidermal *s. corneum* samples were studied in present work from three body sites of ARCI patients carrying mutations in three different genes, patatin-like phospholipase domain-containing protein 1 *(PNPLA1)*, short chain dehydrogenase/reductase family 9C member 7 *(SDR9C7)* and transglutaminase 1 *(TGM1)*. The results showed marked alterations in the proteome resulting from each genetic defect, thus suggesting not only a novel approach for the diagnosis of ARCI, but also potentially offering insight into disease pathogenesis that could eventually aid in therapeutic efforts.

2. Materials and methods

2.1. Tape circles collection

Approval from the Institutional Review Board of Quaid-i-Azam University, Islamabad, Pakistan (IRB#216) and the University of California, Davis (IRB#217868-14) was obtained prior to commencement of the study, and informed consent was obtained from all the participating individuals. Subjects affected with ARCI underlying mutations in the genes *TGM1* (1 female, 2 male subjects), *SDR9C7* (1 male, 2 female subjects) and *PNPLA1* (4 male subjects), as well as 7 normal control individuals (5 females, 2 males) were recruited from different areas of Pakistan. The patients with each given condition were from the same family and had the same gene mutation. Thus, a small contribution of inter-family differences to the results cannot be discounted. Surface corneocyte samples from three bodily sites (forehead, forearm and shin of the leg) were collected for protein profiling using CuDerm D101 D-squame adhesive circles. These tape circles (2.2 cm) were applied on the studied skin sites, pressed with the thumb in a circular motion to enhance keratinocyte adherence, and then stripped off with forceps. The tape circles, three for each sample, were placed in 15 ml sterile conical polystyrene centrifuge tubes so that the sticky surface, carrying the keratinocytes, faced the center of the tube.

2.2. Sample processing

Tape circles with attached keratinocytes were held in 2% sodium dodecyl sulfate – 0.1 M sodium phosphate buffer (pH 7.8) overnight, allowing the keratinocytes to elute from the circles and settle at the bottoms of the tubes. The keratinocytes from each sample were transferred to a clean microfuge tube followed by centrifugation. The supernatant was discarded and the pellet was washed twice by re-suspension in 2% sodium dodecanoate – 0.1 M NH_4HCO_3 followed by centrifugation. The resulting pellet was then re-suspended in 0.4 ml of 2% SD – 0.1 M NH_4HCO_3. After addition of dithioerythritol to 50 mM, samples were incubated at 95ºC for 15 min followed by an hour at 37ºC. Sulfhydryls were alkylated with iodoacetamide (100 mM) with

stirring for 45 min in the dark. Sodium dodecanoate was removed by extracting three times with 700 µL of ethyl acetate after adjusting the pH to ~3 with trifluoroacetic acid. The aqueous layer was readjusted to pH ~8.5 with 2.5 µL of concentrated ammonium hydroxide and 20 µL of 1M NH_4HCO_3 before addition of 20 µg of reductively methylated trypsin [9] for protein digestion. Digestion was continued for 3 days with daily additions of 20 µg of trypsin. The samples were clarified by centrifugation and stored frozen until analysis.

2.3 Mass spectrometry and database searching

Peptides were subjected to LC-MS/MS analysis on a Thermo Scientific Q Exactive Plus Orbitrap mass spectrometer provided with Proxeon nanospray and Proxeon Easy-nLC II HPLC essentially as previously described [10]. The MS/MS generated spectral data were searched with Uniprot Human Proteome database (7/13/2017), a database of common laboratory contaminants (www.thegpm.org/crap) and an equal number of reverse decoy sequences, employing X! Tandem (The GPM, thegpm.org; version X! Tandem Alanine (2017.2.1.4)) set up for trypsin as the digestion enzyme. The search was performed with the fragment ion mass tolerance of 20 ppm and parent ion tolerance of 20 ppm initially with subsequent screening at 5 ppm, cysteine carbamidomethylation as fixed modification, and with N-terminal ammonia loss, N-terminal glutamate or glutamine pyrolysis (Glu/Gln → pyro-Glu), aspargine and glutamine deamidation, and oxidation or dioxidation of methionine and tryptophan as variable modifications.

Peptides and proteins identified by MS/MS were validated using Scaffold (version Scaffold_4.8.2, Proteome Software Inc., Portland). Peptide identifications found to be established at >95% probability by Scaffold LFDR algorithm were accepted, while the protein identifications were accepted if corroborated at >99% probability with at least two identified peptides. This stringent criterion reduced the peptide decoy FDR to 0.1% and protein decoy FDR

to 1.3%. Proteins that could not be differentiated by MS/MS analysis solely, due to presence of similar peptides, were clustered to satisfy parsimony principles. As previously observed [11], numerous semi-tryptic peptides were obtained in the digests (≈40% of the total). They showed the same protein identification specificity in this work as full tryptic peptides judging by distribution between given proteins and clusters and by estimated false discovery rate. The weighted spectral count values for the proteins were compared to the spectral counts of exclusive peptides (peptides belonging to only one protein), and the proteins with numerous weighted counts but no or very few exclusive peptides were omitted from the analysis. The raw data, peak lists and Scaffold file used in the study are available in the Massive Proteomics repository (massive.ucsd.edu/ #MSV000082828, reviewer password Ichthyosis082018) and ProteomeExchange (http://www.proteomexchange.org/ #PXD010814).

2.4 Statistical analysis

Proteins with average level less than 1 count were filtered, leaving 301 proteins. Normalization factors were calculated using TMM normalization as implemented in the Bioconductor package edgeR [12]. Differential abundance analyses were conducted using a two-factor ANOVA model in the limma-voom Bioconductor pipeline [13], including effects for group, location, and the group-location interaction. Analyses were conducted using R, version 3.4.1.

3. Results

3.1. Protein profile variation at different locations in control

Proteomic analysis of the epidermal samples from patients and controls resulted in identification of a total of 454 proteins, of which 301 were prevalent enough for statistical analysis. In unaffected epidermis, keratins were prominent in the protein profile at each site, accounting for

the large majority of the material judging by spectral counts. The profiles of proteins from the sites differed, but those from the forearm and leg were more similar to each other than to that from the forehead. Two-way comparisons of the spectral counts of each identified protein provided a measure of the degree of difference among the profiles at the three sites. The arm and leg profiles were essentially indistinguishable, while the forehead profile exhibited 136 and 139 protein differences from those of arm and leg, respectively. Samples from forehead had half the level of KRT2, a major component, which was balanced by relatively higher levels of 90% of the other proteins that differed in level, each much less prevalent. The relative levels of a score of keratins and a comparable number of other proteins are illustrated in Supplementary Figure S1.

3.2 Proteins differing in levels in patients vs control

Two-way comparisons of individual protein levels between the three groups (*PNPLA1*, *SDR9C7*, *TGM1*) and controls were made from the three anatomic sites above to examine the proteome disturbances in these scaly phenotypes. Results showing the fold changes from control levels for nearly 180 proteins for which the changes were statistically significant are tallied in Supplementary Table S1 and are illustrated in a heatmap permitting rapid visualization (Supplementary Figure S2). For reference, Supplementary Table S2 is a list of gene abbreviations and associated protein names. Analysis of the profiles revealed the *PNPLA1* group to be the most diverged from normal, with 138 proteins having significantly different levels, followed closely by *SDR9C7* (114 proteins) and more distantly by *TGM1* (36 proteins) samples (Figure 1a). The groups exhibited protein alterations overlapping with each other as well as exclusive to the groups (Figure 1b). The direction of change was the same in all the proteins shared by the groups except for four proteins (ARG1, CYSRT1, PSMA7, TGM3) in *SDR9C7* and *PNPLA1* samples. *PNPLA1* and *SDR9C7* groups exhibited approximately equal numbers

(45% and 55%, respectively) of proteins increased vs decreased; however, in the *TGM1* group two-thirds of the altered proteins had increased levels compared to control. Surprisingly, among all the keratins whose levels were altered in the disease groups, 19 of 24 were lower in the ichthyosis samples, and all 13 keratin associated proteins that differed were lower as well.

Profiles were examined to determine the degree to which changes in expression level were common among the three patient groups. 20 proteins were found to be consistently increased or decreased in level. KRT16, expressed in keratinocytes in hyperproliferative states such as wound healing and inflammation [14,15], was found to be elevated, whereas KRT77 and three KRTAP9 family members were suppressed. Besides keratins, junctional proteins (JUP and DSP) and some cornified envelope components (SPRR1A, SPRR2D, LCE3D, POF1B, and FLG) were also elevated in the disease groups, while TGM1 was among the 5 proteins suppressed, dramatically in the *TGM1* defective samples and by about one-third in the others. Proteins that were increased included FABP5, HSPB1, IDE, TPM3, CANX, PRDX1 and VCL (Figure 1c). Supplementary Figure S3 shows weighted spectral count data corresponding to the protein ratios in Figure 1c.

The remarkable overlap of 52 proteins altered in the same direction in both *PNPLA1* and *SDR9C7* samples is illustrated in Figure 2, which presents the proteins increased or decreased by at least a factor of two. Those suppressed include 5 keratins, two histones and the lipoxygenases ALOXE3 and ALOX12B. SDR9C7 is virtually absent in the *SDR9C7* samples as expected, but appears a third lower in the *PNPLA1* samples than in the controls. Among the variety of proteins found at higher levels are two SPRRs, two S100A proteins and IL36. The 56 proteins found to be altered only in the *PNPLA1* samples, mostly decreased in level, included 6 keratins and two keratin associated proteins, while KRT17 and EVPL were increased (Figure 3a). By contrast, proteins with increased levels were prominent in the *SDR9C7* samples, including CALML5

critical for keratinocyte differentiation [16], while several LCE family members were decreased (Figure 3b). Levels of relatively few proteins (7) were altered in the *TGM1* samples, among which KRT9, LOR and PRDX2 were increased, while NCCRP1 was decreased (Figure 4). The overlap between the *TGM1* samples and either *PNPLA1* (5) or *SDR9C7* (4) samples was small, with SPRR2A, ACTB and HRNR stimulated in the former and AHNAK in the latter.

3.3. Comparison of protein profiles at different anatomic sites

Profiles of subjects and controls were analyzed to find the site specificity of the response. Consistent with the collective results, the profiles at arm and leg were most divergent from normal for the *PNPLA1* group followed by *SDR9C7*, whereas *TGM1* samples illustrated the least divergence from the controls. Forehead profiles, however, displayed the most divergence from normal in the *SDR9C7* group followed by *PNPLA1* and *TGM1* deficient subjects. *PNPLA1* and *SDR9C7* samples shared a large number of protein differences, consistent with their similar phenotypic appearance. Some protein alterations were common to the three patient groups at leg and arm but none at forehead (Figure 5), which could reflect the absence of scales on forehead in the *TGM1* group (Table 1). Thus, the degree of divergence from normal in protein profiles appears influenced by anatomic site as well as the disease manifestation.

3.4 Proteome to phenotype correlation

Connecting a disease genotype to the phenotype in general is difficult, including for ichthyoses arising from *PNPLA1* defects [17,18]. Present results indicate the observed proteomic differences from normal, a state between genotype and phenotype, were dependent primarily on the genetic lesion. To analyze the relation of proteome to phenotype, the lesions sampled from subjects were classified according to scale color, size and density. As is seen in Table 1, the

divergence of protein profiles from normal was least at sites where the scales were dense, thick and dark compared to sites having finer and lighter scales. Consistent with this observation, the phenotype appeared more severe in the *TGM1* group with large dark brown and thick scales, followed by *SDR9C7* and then *PNPLA1*, while the number of altered protein levels increased in this direction. Thus, quantitative evaluation of lesions in addition to visual inspection would help to judge departure from normal and the degree of remission as a result of treatment.

4. Discussion

Proteomic analysis of corneocytes from several anatomic sites revealed prominent variations in their composition. The proteomes of arm and leg samples were most similar in the control individuals but exhibited striking differences from forehead. Such differences, previously observed in less detail [8], could reflect the thinner *s. corneum* in forehead (9 cell layers) compared to that of arms and legs (~25 cell layers) [19]. In any case, the data emphasize the need to compare the proteome of affected sites with corresponding sites in controls.

Proteomic profiling of the three ARCI types revealed marked differences in the proteomes resulting from defects in different genes that perturb different keratinization pathways. Keratinization is a highly organized and precisely timed process forming the cutaneous barrier integral to terrestrial life. Defects in barrier function disturb the cellular machinery, triggering responses to compensate or retain barrier functions [20]. Imbalanced and incessant (due to their genetic nature) homeostatic responses to the barrier defects result in hyperkeratinized epidermis sometimes accompanied by erythroderma reflected in elevated cytokine levels [21]. While the differences in response likely reflect the specific genetic defects, overlaps in response may reflect common elements in the compensation to alleviate compromised barrier functions. For instance, we speculate that reduction in KRT77 (found in cells lining eccrine gland ducts) in all

three sample types could lead to or reflect reduction in eccrine gland effectiveness responsible for hypohidrosis, limiting trans-epidermal water loss. Although these conditions shared a substantial number of protein changes, present findings indicate the distinct proteomic variations in the diseased areas to be manifestations specific to the primary defects. Finding protein changes characteristic of certain genetic deficiencies may permit targeted, more rapid proteomic assays [22]. Initial efforts to identify pathways with perturbations specific to the genetic defects (using Ingenuity Pathway Analysis, for example) have not been successful but have raised interesting possibilities for further investigation. Compilation of data beyond the limited number of current subjects is anticipated to facilitate pathway identifications.

The striking difference in magnitude of proteomic response between the *PNPLA1* and *SDR9C7* compared to *TGM1* samples likely reflects major imbalances in epidermal lipids in the former. In mice with ablated *PNPLA1* and in humans lacking PNPLA1 activity, the lipid profile is clearly altered [23-25]. Although studied in less detail, defective SDR9C7 activity appears to result in ichthyosis with reduced intercellular lipid [26]. Since a wide variety of interconnected intracellular signaling pathways are subject to alteration by an altered lipid environment, clarifying the genotype to phenotype connections is likely to be challenging. Indications of altered pathways from transcriptional analysis, including possible activation of PPARδ with consequent increase in FABP5 and SPRR1B levels, could help rationalize aspects of the phenotype [25]. Proteomic analysis of alterations in protein levels in superficial corneocytes may provide valuable complementary information. In the meantime, treatment by approximating the normal epidermal environment with lipid supplements appears promising [24].

Recent work exploring alterations in various epidermal differentiation markers reveals changes measured by transcriptional analysis, immunohistochemistry and immunoblotting. In such

249 studies, LOR has been consistently reported at lower levels in *PNPLA1* epidermis, while FABP5
250 was higher, and FLG and IVL have been reported as increased or without change depending on
251 the method. In *SDR9C7* epidermis, LOR appeared unchanged, while INV and FLG appeared at
252 higher level, possibly due to increased stratification [27]. In present work, FLG and FABP5 were
253 found to be increased in all three conditions, while LOR was increased only in *TGM1* samples,
254 and IVL was increased in *PNPLA1* and *SDR9C7* samples. Such discrepancies likely reflect the
255 specifics of the methods, but a small contribution from inter-individual differences cannot be
256 dismissed. Proteomic analysis at least reports levels at the conclusion of processing steps after
257 gene expression. Not as comprehensive as DNA microarray or next generation sequencing,
258 protein profiling nevertheless gives a view of numerous gene products. For example, although
259 their impact is uncertain, changes that could contribute to the observed phenotypes include
260 reductions in TGM1, ALOX3E, ALOX12B and SPINK5 in *PNPLA1* and *SDR9C7* samples.
261 Whether alterations in levels of prominent components of cross-linked envelopes affect the
262 envelope properties is plausible but uncertain, since their degree of incorporation is not directly
263 related to total protein amount, and some proteins appear able to compensate for loss of others
264 [28]. In any case, examination of a broader spectrum of patients with the same and different
265 specific inactivating mutations will be important to characterize consistent alterations in protein
266 levels.

267 The following are supplementary data related to this article.

268 Table S1. Proteins differing from Control (Con) samples. For each category are shown the
269 values for fold change (FC) and weighted spectral counts (WSC) for control samples. Proteins
270 with the yellow highlight, with at least 2 FC and 10 WSC in control or ichthyosis samples, are

displayed in the figure corresponding to the category (PNP = PNPLA1, SDR = SDR9C7, TGM = TGM1).

Table S2. Gene abbreviations and protein names.

Fig. S1. Ratios of protein levels in control samples from forehead to those from leg and arm. Illustrated are those with ratios of weighted spectral counts with at least a two fold difference in forehead compared to arm and leg (averaged with error bars showing the range for arm and leg). The dashed line indicates a ratio of 1. Each protein had >20 spectral counts in forehead samples.

Fig. S2. Heatmap showing all the proteins altered in the disease groups arranged in alphabetical order. The map was generated using the Expression tool of Heatmapper software [30]. Red color indicates down regulation, while green color indicates up regulation of protein in the samples. Intensities of the colors are directly proportional to the degree of up or down regulation.

Fig. S3. Weighted spectral counts of the 20 proteins common to SDR9C7, PNPLA1, and TGM1 groups. The error bars represent standard deviations from the mean.

Fig. S4. Images of typical scaling patterns.

Conflict of interest

The authors declare no conflict of interest.

References

[1] Takeichi T, Akiyama M. Inherited ichthyosis: Non-syndromic forms. J Dermatol 2016;43:242-251

[2] Akiyama M. Corneocyte lipid envelope (CLE), the key structure for skin barrier function and ichthyosis pathogenesis. J Dermatol Sci 2017;88:3-9

[3] Heinz L, Kim GJ, Marrakchi S, Christiansen J, Turki H, Rauschendorf MA, Lathrop M, Hausser I, Zimmer AD, Fischer J. Mutations in SULT2B1 cause autosomal-recessive congenital ichthyosis in humans. Am J Hum Genet 2017;100:926-939.

[4] Elias PM, Williams ML, Feingold KR. Abnormal barrier function in the pathogenesis of ichthyosis: Therapeutic implications for lipid metabolic disorders. Clin Dermatol 2012;30:311-322

[5] Richard G. Autosomal recessive congenital ichthyosis. In Adam MP, Ardinger HH, Pagon RA, Wallace SE, Bean LJH, Amemiya A, editors. GeneReviews. University of Washington, Seattle; 2017.

[6] Youssef G, Ono M, Brown SJ, Kinsler VA, Sebire NJ, Harper JI, O'shaughnessy RF. Identifying a hyperkeratosis signature in autosomal recessive congenital ichthyosis: Mdm2 inhibition prevents hyperkeratosis in a rat ARCI model. J Invest Dermatol 2014;134:858-861

[7] Li H, Loriè EP, Fischer J, Vahlquist A, Törmä H. The expression of epidermal lipoxygenases and transglutaminase-1 is perturbed by NIPAL4 mutations: indications of a common metabolic pathway essential for skin barrier homeostasis. J Invest Dermatol 2012;132:2368-2375

[8] Rice RH, Bradshaw KM, Durbin-Johnson BP, Rocke DM, Eigenheer RA, Phinney BS, Schmuth M, Gruber R. Distinguishing ichthyoses by protein profiling. PLoS One 2013;8(10):e75355

[9] Rice RH, Means GE, Brown WD. Stabilization of bovine trypsin by reductive methylation. Biochim Biophys Acta 1977;492:316-321

[10] Rice RH, Durbin-Johnson BP, Salemi M, Schwartz ME, Rocke DM, Phinney BS. Proteomic profiling of Pachyonychia congenita plantar callus. J Proteomics 2017;165:132-137

[11] Lee YJ, Rice RH, Lee YM. Proteomic analysis of human hair shaft: From protein identification to posttranslational modification. Molec Cell Proteom 2006;5:789-800

[12] Robinson MD, McCarthy DJ, Smyth GK. edgeR: a Bioconductor package for differential expression analysis of digital gene expression data. Bioinformatics 2010;26:139-140

[13] Ritchie ME, Phipson B, Wu D, Hu Y, Law CW, Shi W, Smyth GK. limma powers differential expression analyses for RNA-sequencing and microarray studies. Nucl Acids Res 2015;43(7):e47.

[14] Bhawan J, Bansal C, Whren K, Schwertschlag U, Group I-PS. K16 expression in uninvolved psoriatic skin: a possible marker of pre-clinical psoriasis. J Cutan Pathol 2004;7:471-476

[15] Lessard JC, Piña-Paz S, Rotty JD, Hickerson RP, Kaspar RL, Balmain A, Coulombe PA. Keratin 16 regulates innate immunity in response to epidermal barrier breach. Proc Natl Acad Sci USA 2013;110:19537-19542

[16] Sun BK, Boxer LD, Ransohoff JD, Siprashvili Z, Qu K, Lopez-Pajares V, Hollmig ST, Khavari PA. CALML5 is a ZNF750- and TINCR-induced protein that binds stratifin to regulate epidermal differentiation. Genes Develop 2015;29:2225-2230

[17] Boyden LM, Craiglow BG, Hu RH, Zhou J, Browning J, Eichenfield L, Lim YL, Luu M, Randolph LM, Ginarte M, Fachal L. Phenotypic spectrum of autosomal recessive congenital ichthyosis due to PNPLA1 mutation. Br J Dermatol 2017;177:319-322

[18] Vahidnezhad H, Youssefian L, Saeidian AH, Zeinali S, Mansouri P, Sotoudeh S, Barzegar M, Mohammadi-asl J, Karamzadeh R, Abiri M, McCormick K. Gene-targeted next generation sequencing identifies PNPLA1 mutations in patients with a phenotypic spectrum of autosomal recessive congenital ichthyosis: The impact of consanguinity. J Invest Dermatol 2017;137:678-685

[19] Ya-Xian Z, Suetake T, Tagami H. Number of cell layers of the stratum corneum in normal skin – relationship to the anatomical location on the body, age, sex and physical parameters. Arch Dermatol Res 1999;291:555-559

[20] Schmuth M, Gruber R, Elias PM, Williams ML. Ichthyosis update: towards a function-driven model of pathogenesis of the disorders of cornification and the role of corneocyte proteins in these disorders. Adv Dermatol 2007;23:231-256

[21] Czarnowicki T, He H, Leonard A, Malik K, Magidi S, Rangel S, Patel K, Ramsey K, Murphrey M, Song T, Estrada Y. The major orphan forms of ichthyosis are characterized by systemic T-cell activation and Th-17/Tc-17/Th-22/Tc-22 polarization in blood. J Invest Dermatol 2018;138:2157-2167

[22] Reisdorph N, Armstrong M, Powell R, Quinn K, Legg K, Leung D, Reisdorph R. Quantitation of peptides from non-invasive skin tapings using isotope dilution and tandem mass spectrometry. J Chromatography B 2017;1084:132-140

[23] Pichery M, Hucheng A, Sandhoff R, Severino-Freire M, Zaafouri S, Opalka L, Levade T, Soldan V, Bertrand-Michel J, Lhuillier E, Serre G. PNPLA1 defects in patients with autosomal recessive congenital ichthyosis and KO mice sustain PNPLA1 irreplaceable function in epidermal omega-O-acylceramide synthesis and skin permeability barrier. Hum Mol Genet 26(10), 1787-1800.

[24] Grond S, Eichmann TO, Dubrac S, Kolb D, Schmuth M, Fischer J, Crumrine D, Elias PM, Haemmerle G, Zechner R, Lass A. PNPLA1 deficiency in mice and humans leads to a defect in the synthesis of omega-O-acylceramides. J Invest Dermatol 2017;137:394-402

[25] Hirabayashi T, Anjo T, Kaneko A, Senoo Y, Shibata A, Takama H, Yokoyama K, Nishito Y, Ono T, Taya C, Muramatsu K. PNPLA1 has a crucial role in skin barrier function by directing acylceramide biosynthesis. Nature Commun 2017;8:14609

[26] Takeichi T, Nomura T, Takama H, Kono M, Sugiura K, Watanabe D, Shimizu H, Simpson MA, McGrath JA, Akiyama M. Deficient stratum corneum intercellular lipid in a Japanese patient with lamellar ichthyosis with a homozygous deletion mutation in SDR9C. Br J Dermatol 2017;177:e62-e64

[27] Shigehara Y, Okuda S, Nemer G, Chedraoui A, Hayashi R, Bitar F, Nakai H, Abbas O, Daou L, Abe R, Sleiman MB. Mutations in SDR9C7 gene encoding an enzyme for vitamin A

metabolism underlie autosomal recessive congenital ichthyosis. Hum Molec Genet 2016;25:4484-4493

[28] Rice RH, Durbin-Johnson BP, Ishitsuka YI, Salemi M, Phinney BS, Rocke DM, Roop DR. Proteomic analysis of loricrin knockout mouse epidermis. J Proteome Res 2016;15:2560-2566

[29] Oji V, Tadini G, Akiyama M, Blanchet Bardon C, Bodemer C, Bourrat E, Coudiere P, DiGiovanna JJ, Elias P, Fischer J, Fleckman P. Revised nomenclature and classification of inherited ichthyoses: results of the First Ichthyosis Consensus Conference in Sorèze 2009. J Am Acad Dermatol 2010;63:607-641.

[30] Babicki S, Arndt D, Marcu A, Liang Y, Grant JR, Maciejewski A, et al. Heatmapper: web-enabled heat mapping for all. Nucleic Acid Res 2016;44:147-153.

Figure legends

Fig. 1. Proteins altered in level in patient samples vs control. (a) Numbers of altered proteins in two-way comparisons between the three disease groups and control. (b) Venn diagram showing numbers of proteins with altered level shared by the groups and numbers of protein alterations exclusive to the groups. Emphasizing that the direction of change was almost always parallel, numbers following the "/" sign represent the few proteins where the level was altered in the opposite direction. (c) Fold change of proteins with significantly different level common to the three disease groups.

Fig. 2. Proteins altered at least two fold in level in samples from *PNPLA1* and *SDR9C7* patients compared to control. Data represent all three anatomic sites.

Fig. 3. Proteins altered at least two fold in level only in samples from *SDR9C7* (a) and *PNPLA1* (b) patients compared to control. Data represent all three anatomic sites.

Fig. 4. Proteins altered in level at least two fold in samples from *TGM1* patients. Alterations common to *PNPLA1* and *TGM1* patients (left), *TGM1* patients alone (center) and common to *SDR9C7* and *TGM1* patients (right).

Fig. 5. Venn diagrams showing numbers of proteins with altered level shared by the groups at three different anatomic sites. Emphasizing that the direction of change was almost always parallel, numbers following the "/" sign represent the few proteins where the level was altered in the opposite direction.

a

	PNPLA1	SDR9C7	TGM1
Control	138	114	36
PNPLA1	0	55	83
SDR9C7		0	27

b

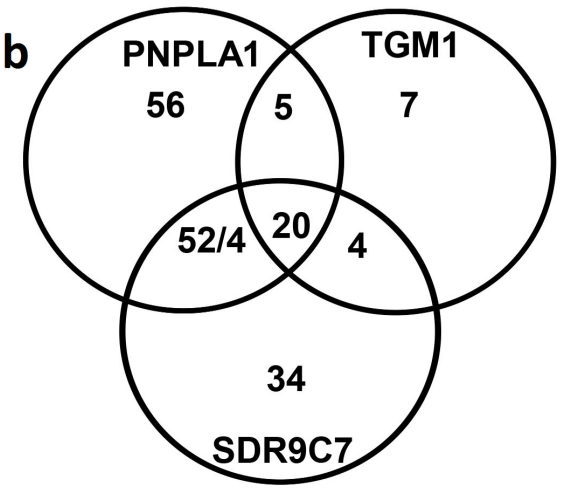

c

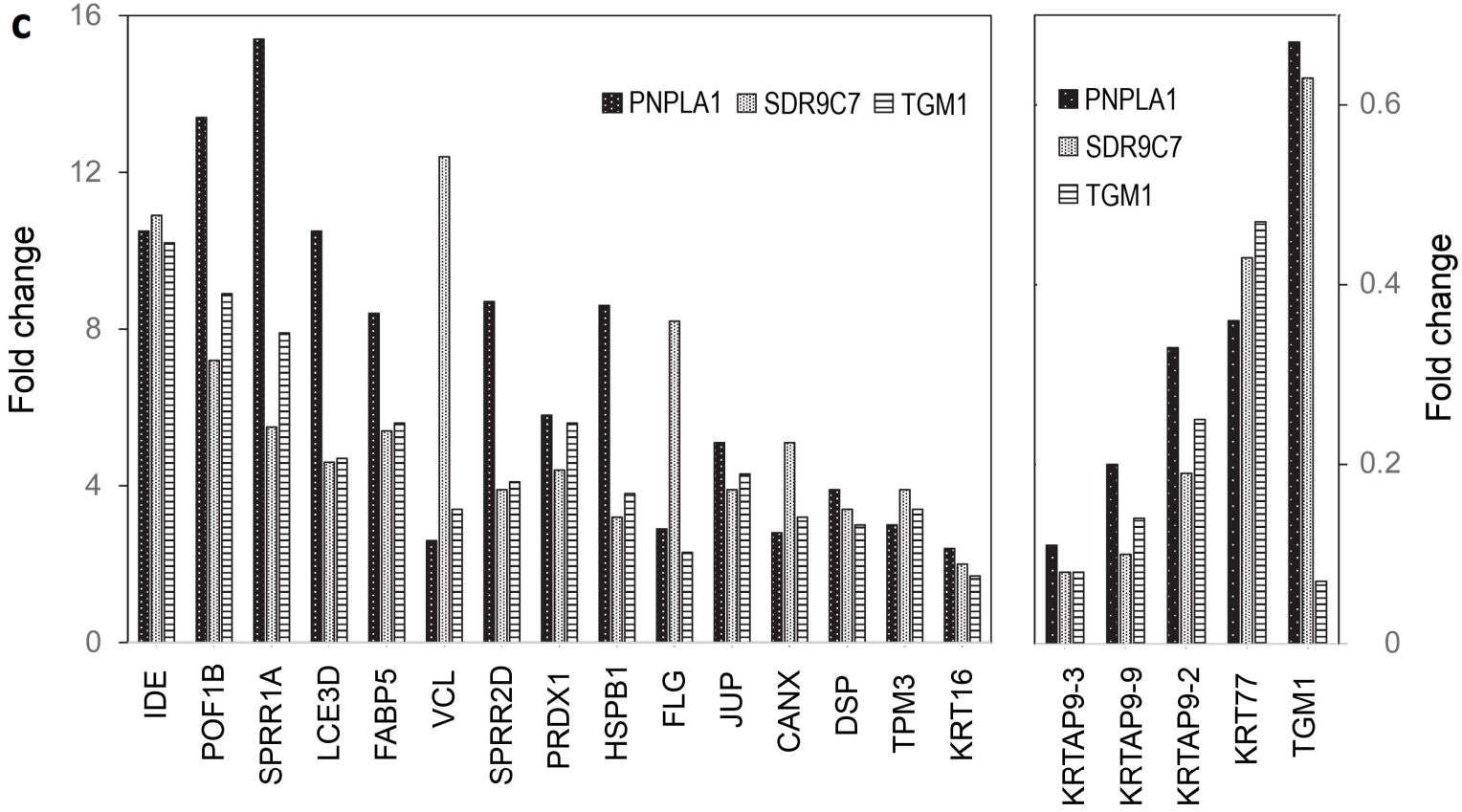

Fold change
12
9
6
3
0
PNPLA1
SDR9C7
S100A8
IVL
MYH9
SPRR2G
IL36
PLEC
MYH14
S100A9
LMNA
LGALS7
HSPA5
SERPINB4
SPRR2F
PKP1
PNPLA1
SDR9C7
VSIG8
S100A3
KRT38
HIST1H4A
KRT35
HIST1H2B1
KRT39
KRT82
ALOXE3
SDR9C7
HAL
KRT84
ALOX12B
0.6
0.4
0.2
0
Fold change

a
SDR9C7
Fold change
0
3
6
9
12
0
0.2
0.4
0.6
Fold change
CALML5
ENO1
VCP
S100A7
TPI1
CTSD
GDI2
EEF2
CSTA
A2ML1
LCE2C
LCE2B
LCE1F
b
PNPLA1
Fold change
0
2
4
6
0
0.15
0.3
0.45
Fold change
EVPL
KRT17
CAT
KRTAP3-1
KRT33B
KRT33A
KRT83
KRT81
KRT32
ECM1
SERPINB1
CAPN
KRT31
KRTAP3-3
GSDMA
AZGP1
LCE1C

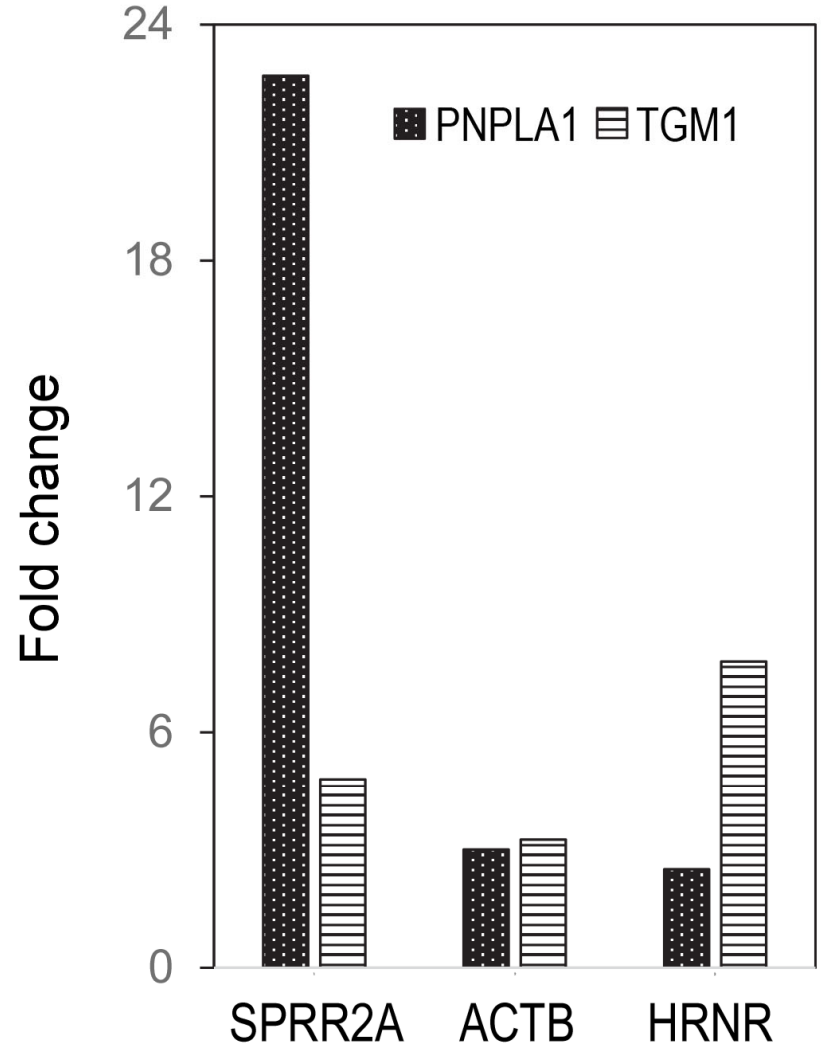
Fold change
24
18
12
6
0
PNPLA1
TGM1
SPRR2A
ACTB
HRNR

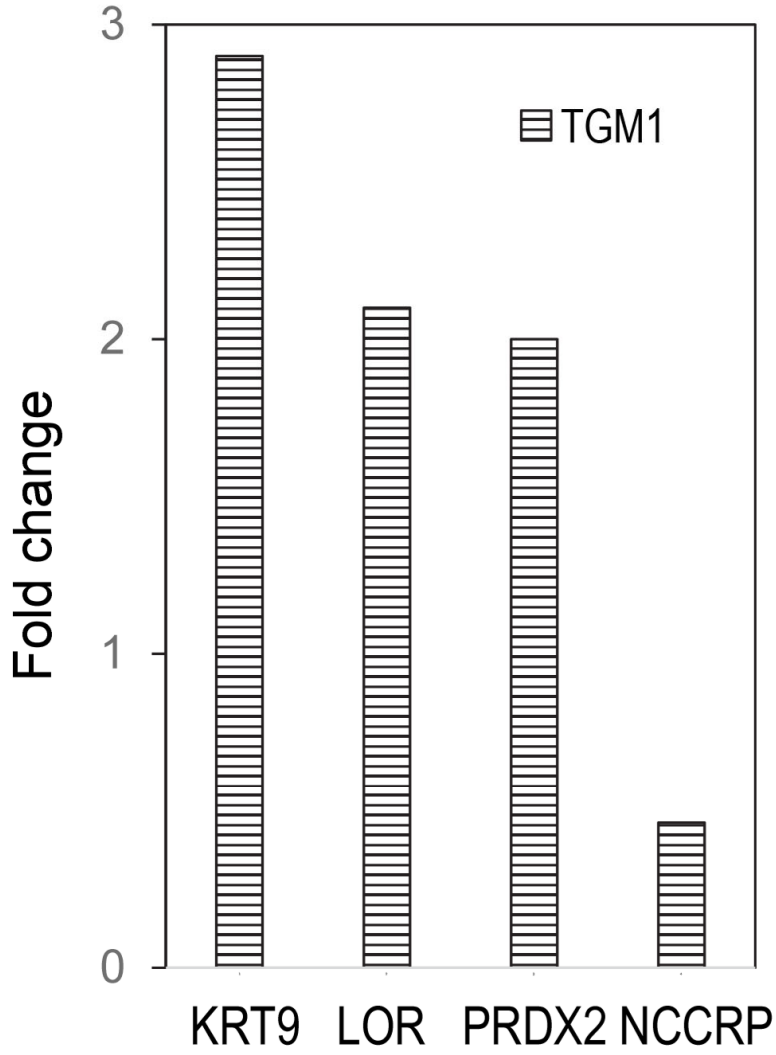
Fold change
3
2
1
0
TGM1
KRT9
LOR
PRDX2
NCCRP1

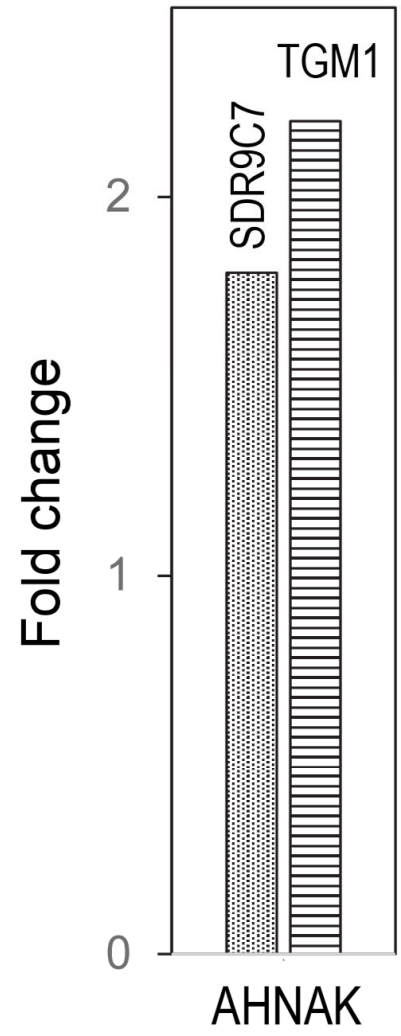
Fold change
2
1
0
SDR9C7
TGM1
AHNAK

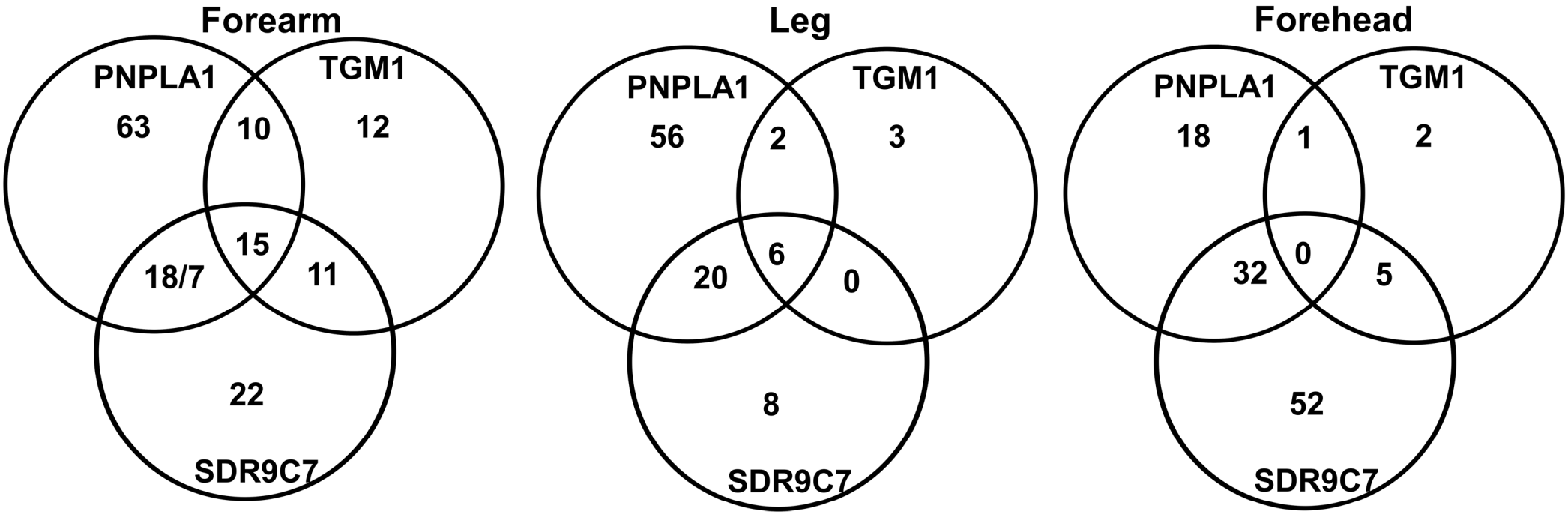
Forearm
PNPLA1
TGM1
63
10
12
15
18/7
11
22
SDR9C7
Leg
PNPLA1
TGM1
56
2
3
6
20
0
8
SDR9C7
Forehead
PNPLA1
TGM1
18
1
2
0
32
5
52
SDR9C7

Table S1. Proteins differing from Control (Con) samples. For each category are shown the values for fold change (FC) and weighted spectral counts (WSC) for control samples. Proteins with the yellow highlight, with at least 2 FC and 10 WSC in control or ichthyosis samples, are displayed in the figure corresponding to the category (PNP = PNPLA1, SDR = SDR9C7, TGM = TGM1).

Figure 1

All3	FC	FC	FC	WSC
Protein	**PNP**	**SDR**	**TGM**	**Con**
CANX	2.8	5.1	3.2	0.7
DSP	3.9	3.4	3	240
FABP5	8.4	5.4	5.6	4.4
FLG	2.9	8.2	2.3	197
HSPB1	8.6	3.2	3.8	6.3
IDE	10.5	10.9	10.2	10.4
JUP	5.1	3.9	4.3	104
KRT16	2.4	2	1.7	72
KRT77	0.36	0.43	0.47	190
KRTAP9-2	0.33	0.19	0.25	3.6
KRTAP9-3	0.11	0.08	0.08	24
KRTAP9-9	0.2	0.1	0.14	12
LCE3D	10.5	4.6	4.7	2.1
POF1B	13.4	7.2	8.9	28
PRDX1	5.8	4.4	5.6	8.5
SPRR1A	15.4	5.5	7.9	5.2
SPRR2D	8.7	3.9	4.1	9.4
TGM1	0.67	0.63	0.07	78
TPM3	3	3.9	3.4	1
VCL	2.6	12.4	3.4	0.8

Figure 5

PNP/TGM1	FC	FC	WSC
Protein	**PNP**	**TGM**	**Con**
ACTB	3	3.25	17
FASN	2.7	4.7	0.4
HRNR	2.5	7.8	9.6
KPRP	0.73	0.73	362
SPRR2A	22.7	4.8	6

TGMonly	FC	WSC
Protein	**TGM**	**Con**
KRT1	0.83	1875
KRT9	2.9	129
LOR	2.1	28
NCCRP1	0.46	12.6
PLD3	0.48	0.8
PRDX2	2	14.8
YOD1	0.27	5

SDR/TGM	FC	FC	WSC
Protein	**SDR**	**TGM**	**Con**
AHNAK	1.8	2.2	44
HARS	5.1	3.8	0.8
KRT36	0.27	0.34	8.6
SPRR3	0.47	0.44	1.7

Figure 2

PNP/SDR	FC	FC	WSC
Protein	**PNP**	**SDR**	**Con**
ALOX12B	0.49	0.59	76
ALOXE3	0.3	0.32	45
ARG1	0.43	1.6	
C11orf54	0.3	0.32	3
CKMT1A	2.7	5.4	0.4
CYSRT1	7.2	0.48	
DCD	0.23	0.18	4.3
DSG4	0.42	0.36	7.6
DUSP14	0.52	0.43	2
FLNA	3.1	4.3	0.7
GPNMB	0.29	0.31	5.9
HAL	0.29	0.37	50
HIST1H2BK	0.24	0.26	12
HIST1H4A	0.22	0.22	11.4
HIST2H2AC	0.37	0.36	4.7
HSPA5	3.2	6	3.3
IL36G	4.5	8.2	1
IVL	10.2	7.9	8.9
KRT10	0.89	0.84	2388
KRT14	2	1.5	189
KRT15	0.7	0.69	40
KRT2	0.72	0.73	1882
KRT35	0.2	0.26	24
KRT38	0.15	0.26	32
KRT39	0.27	0.28	11.7
KRT40	0.28	0.23	4.4
KRT6A	1.9	1.5	58
KRT80	0.8	0.76	65
KRT82	0.29	0.27	44
KRT84	0.39	0.45	24
KRTAP11-1	0.3	0.34	3.4
KRTAP16-1	0.32	0.29	8.3
KRTAP2-2	0.23	0.19	4
KRTAP24-1	0.43	0.23	3.2
KRTAP4-3	0.29	0.35	4.1
LCE3E	4	2.9	0.24
LGALS7	6.4	4	11.2
LMNA	2.9	8.4	4.4
LRRC15	0.36	0.26	7
MYH14	5.6	6.4	2.4
MYH9	6.5	9.3	6.4
PKP1	4	2.5	19
PLEC	4.8	7.5	4
PSMA7	0.38	3	
S100A2	3.3	2.6	1.5
S100A3	0.23	0.1	10.2
S100A8	12.2	9	11.9
S100A9	5.4	6.5	15.7
SDR9C7	0.62	0.02	14.6
SERPINB4	3.9	4.4	8.5
SPINK5	0.47	0.46	1.8
SPRR2F	4	2.9	12
SPRR2G	10.5	5.2	20
TGM3	0.47	1.7	
VSIG8	0.2	0.13	14

Figure 3

PNPonly	FC	WSC
Protein	**PNP**	**Con**
ALAD	0.3	1.5
ALDH2	3.1	0.1
ASAH1	0.27	2.5
AZGP1	0.34	16.7
CAPN1	0.22	13.4
CASP14	0.51	40
CAT	0.08	29
CPNE3	0.51	19.3
CRCT1	2	4.7
DSC1	0.64	78
DSG1	0.79	246
ECM1	0.21	26
EEF1A2	4.3	2
EVPL	5.6	2.8
GAPDH	0.58	35
GDA	3.3	1.5
GGH	0.37	3.4
GLRX	0.26	7.9
GLUL	8.9	0.2
GSDMA	0.29	22.8
HSPA1A	2.7	1.5
HSPD1	4.8	0
IDH1	0.4	1.7
KRT17	2.2	40
KRT31	0.23	131
KRT32	0.21	36
KRT33A	0.17	111
KRT33B	0.16	140
KRT81	0.18	49
KRT83	0.18	46
KRTAP13-2	0.45	6.3
KRTAP3-1	0.15	16.5
KRTAP3-3	0.27	11
LCE1C	0.48	25
LCE1D	0.13	7
LCE3A	3.8	0.1
LCE5A	0.25	2.9
LCN2	7.4	0
LGALS3	0.43	4.9
LY6D	4.1	0.2
MSN	2.4	0.2
PAICS	0.35	6.3
PI3	3.1	0
PSAP	0.2	3.8
RACK1	2.4	0.2
RPS3	2.76	0.4
S100A11	2	4.1
S100A14	1.6	21
SERPINB12	0.21	12.6
SERPINB8	0.28	3.4
SLC25A5	3.8	0
STS	0.48	1
SULT2B1	1.85	0.2
TROVE2	0.36	2
UncharProt	3.86	3.3
VDAC2	3.85	1.9

Figure 4

SDRonly	FC	WSC
Protein	**SDR**	**Con**
A2ML1	2.8	25
ALDOA	4.3	2
ANXA2	1.3	55
BLMH	1.6	50
CALML5	12.9	2
CSTA	3	8
CTSB	2.8	1.4
CTSD	4.7	9.5
EEF2	3.2	8
ENO1	9.5	16
GDI2	3.9	4
GOT1	3.3	1.6
HEPHL1	0.35	1.5
HIST1H1E	0.47	2
IGKC	1.8	0.2
KRTAP4-11	0.2	7.7
KRTAP7-1	0.41	1
LCE1F	0.5	19
LCE2A	0.37	6
LCE2B	0.35	19
LCE2C	0.33	11
PMEL	0.32	1.8
PNP	3.6	1.1
PSMA4	3.8	0.9
PSMA6	3.4	1
RNASE7	0.52	15.5
RPN1	2.4	0.3
S100A7	5.8	7.8
SERPINB2	2.8	0.5
TALDO1	3.3	0.6
TKT	4.6	1.5
TPI1	4.8	14
VCP	7.8	4.6
XP32	0.63	97

Table S2. Gene abbreviations and protein names.

Gene Abbreviation	Protein Name
A2ML1	Alpha-2-Macroglobulin Like 1
ACTB	Beta-Actin
AHNAK	Desmoyokin
ALAD	Delta-Aminolevulinate Dehydratase
ALDH2	Aldehyde Dehydrogenase
ALDOA	Class I Fructose-Bisphosphate Aldolase
ALOX12B	Arachidonate 12-Lipoxygenase, 12R Type
ALOXE3	Arachidonate Lipoxygenase 3
ANXA2	Annexin A2
ARG1	Arginase 1
ASAH1	N-Acylsphingosine Amidohydrolase 1
AZGP1	Zinc-Alpha-2-Glycoprotein
BLMH	Bleomycin Hydrolase
C11orf54	Chromosome 11 Open Reading Frame 54
CALML5	Calmodulin-Like Protein 5
CANX	Calnexin
CAPN1	Calpain 1
CASP14	Caspase 14
CAT	Chloramphenical Acetyl Transferase
CKMT1A	Creatine Kinase, Mitochondrial 1A
CPNE3	Copine 3
CRCT1	Cysteine Rich C-Terminal 1
CSTA	Cystatin A
CTSB	Cathepsin B
CTSD	Cathepsin D
CYSRT1	Cysteine Rich Tail 1
DCD	Dermicidin
DSC1	Desmocollin-1
DSG1	Desmoglein-1
DSG4	Desmoglein 4
DSP	Desmoplakin
DUSP14	Dual Specificity Phosphatase 14
ECM1	Extracellular Matrix Protein 1
EEF1A2	Elongation Factor 1-Alpha 2
ENO1	Enolase 1

EVPL	Envoplakin
FABP5	Fatty Acid-Binding Protein 5
FASN	Fatty Acid Synthase
FLG	Filaggrin
FLNA	Filamin A
GAPDH	Glyceraldehyde 3-Phosphate Dehydrogenase
GDA	Guanine Deaminase
GDI2	Gdp Dissociation Inhibitor 2
GGH	Gamma-Glutamyl Hydrolase
GLRX	Glutaredoxin
GLUL	Glutamate-Ammonia Ligase
GOT1	Glutamic-Oxaloacetic Transaminase
GPNMB	Glycoprotein Nmb
GSDMA	Gasdermin A
HAL	Histidine Ammonia-Lyase
HARS	Histidyl-Trna Synthetase
HEPHL1	Hephaestin Like 1
HIST1H1E	Histone Cluster 1 H1 Family Member E
HIST1H2BK	Histone Cluster 1 H2b Family Member K
HIST1H4A	Histone Cluster 1 H4 Family Member A
HIST2H2AC	Histone Cluster 2 H2a Family Member C
HRNR	Hornerin
HSPA1A	Heat Shock Protein Family A
HSPA5	Heat Shock Protein Family A
HSPB1	Heat Shock Protein Family B
HSPD1	Heat Shock Protein Family D
IDE	Insulin Degrading Enzyme
IDH1	Isocitrate Dehydrogenase 1
IGKC	Immunoglobulin Kappa Constant
IL36G	Interleukin-36 Gamma
IVL	Involucrin
JUP	Junction Plakoglobin
KPRP	Keratinocyte Proline Rich Protein
KRT1	Keratin 1
KRT10	Keratin 10
KRT14	Keratin 14
KRT15	Keratin 15

KRT16	Keratin 16
KRT17	Keratin 17
KRT2	Keratin 2
KRT31	Keratin 31
KRT32	Keratin 32
KRT33B	Keratin 33B
KRT35	Keratin 35
KRT36	Keratin 36
KRT38	Keratin 38
KRT39	Keratin 39
KRT40	Keratin 40
KRT44A	Keratin 44A
KRT6A	Keratin 6A
KRT77	Keratin 77
KRT80	Keratin 80
KRT81	Keratin 81
KRT82	Keratin 82
KRT83	Keratin 83
KRT84	Keratin 84
KRT9	Keratin 9
KRTAP11-1	Keratin Associated Protein 11-1
KRTAP13-2	Keratin Associated Protein 13-2
KRTAP16-1	Keratin Associated Protein 16-1
KRTAP2-2	Keratin Associated Protein 2-2
KRTAP24-1	Keratin Associated Protein 24-1
KRTAP3-1	Keratin Associated Protein 3-1
KRTAP3-3	Keratin Associated Protein 3-3
KRTAP4-11	Keratin Associated Protein 4-11
KRTAP4-3	Keratin Associated Protein 4-3
KRTAP7-1	Keratin Associated Protein 7-1
KRTAP9-2	Keratin Associated Protein 9-2
KRTAP9-3	Keratin Associated Protein 9-3
KRTAP9-9	Keratin Associated Protein 9-9
LCE1C	Late Cornified Envelope 1C
LCE1D	Late Cornified Envelope 1D
LCE1F	Late Cornified Envelope 1F
LCE2A	Late Cornified Envelope 2A

LCE2B	Late Cornified Envelope 2B
LCE2C	Late Cornified Envelope 2C
LCE3A	Late Cornified Envelope 3A
LCE3D	Late Cornified Envelope 3D
LCE3E	Late Cornified Envelope 3E
LCE5A	Late Cornified Envelope 5A
LCN2	Lipocalin 2
LGALS3	Galectin-3
LGALS7	Galectin-7
LMNA	Lamin A/C
LOR	Loricrin
LRRC15	Leucine Rich Repeat Containing 15
LY6D	Lymphocyte Antigen 6 Family Member D
MSN	Moesin
MYH14	Myosin Heavy Chain 14
MYH9	Myosin Heavy Chain 9
NCCRP1	Non-Specific Cytotoxic Cell Receptor Protein 1
PAICS	Phosphoribosylaminoimidazole Carboxylase
PI3	Peptidase Inhibitor 3
PKP1	Plakophilin 1
PKP3	Plakophilin 3
PLD3	Phospholipase D Family Member 3
PLEC	Plectin
PMEL	Premelanosome Protein
PNP	Purine Nucleoside Phosphorylase
POF1B	Premature Ovarian Failure Protein 1B
PRDX1	Peroxiredoxin 1
PRDX2	Peroxiredoxin 2
PRSS1	Serine Protease 1
PSAP	Prosaposin
PSMA4	Proteasome Subunit Alpha Type-4
PSMA6	Proteasome Subunit Alpha Type-6
PSMA7	Proteasome Subunit Alpha Type-7
RACK1	Receptor for Activated C Kinase 1
RNASE7	Ribonuclease A Family Member 7
RPN1	Ribophorin 1
RPS3	Ribosomal Protein S3

S100A11	S100 Calcium-Binding Protein A11
S100A14	S100 Calcium-Binding Protein A14
S100A2	S100 Calcium-Binding Protein A2
S100A3	S100 Calcium-Binding Protein A3
S100A7	S100 Calcium-Binding Protein A7
S100A8	S100 Calcium-Binding Protein A8
S100A9	S100 Calcium-Binding Protein A9
SDR9C7	Short Chain Dehydrogenase/Reductase Family 9c Member 7
SERPINA12	Serpin Family A Member 12
SERPINB2	Serpin Family B Member 2
SERPINB4	Serpin Family B Member 4
SERPINB8	Serpin Family B Member 8
SLC25A5	Solute Carrier Family 25 Member 5
SPINK5	Serine Peptidase Inhibitor, Kazal Type 5
SPRR1A	Small Proline Rich Protein 1A
SPRR2A	Small Proline Rich Protein 2A
SPRR2D	Small Proline Rich Protein 2D
SPRR2F	Small Proline Rich Protein 2F
SPRR2G	Small Proline Rich Protein 2G
SPRR3	Small Proline Rich Protein 3
STS	Steroid Sulfatase
SULT2B1	Sulfotransferase Family 2B Member 1
TALDO1	Transaldolase 1
TGM1	Transglutaminase 1
TGM3	Transglutaminase 3
TKT	Transketolase
TPI1	Triosephosphate Isomerase 1
TPM3	Tropomyosin 3
TROVE2	Trove Domain Family Member 2
VCL	Vinculin
VCP	Valosin Containing Protein
VDAC2	Voltage-Dependent Anion-Selective Channel Protein 2
VSIG8	V-Set and Immunoglobulin Domain Containing 8
XP32	Skin-Specific Protein 32
YOD1	Deubiquitinase YOD1

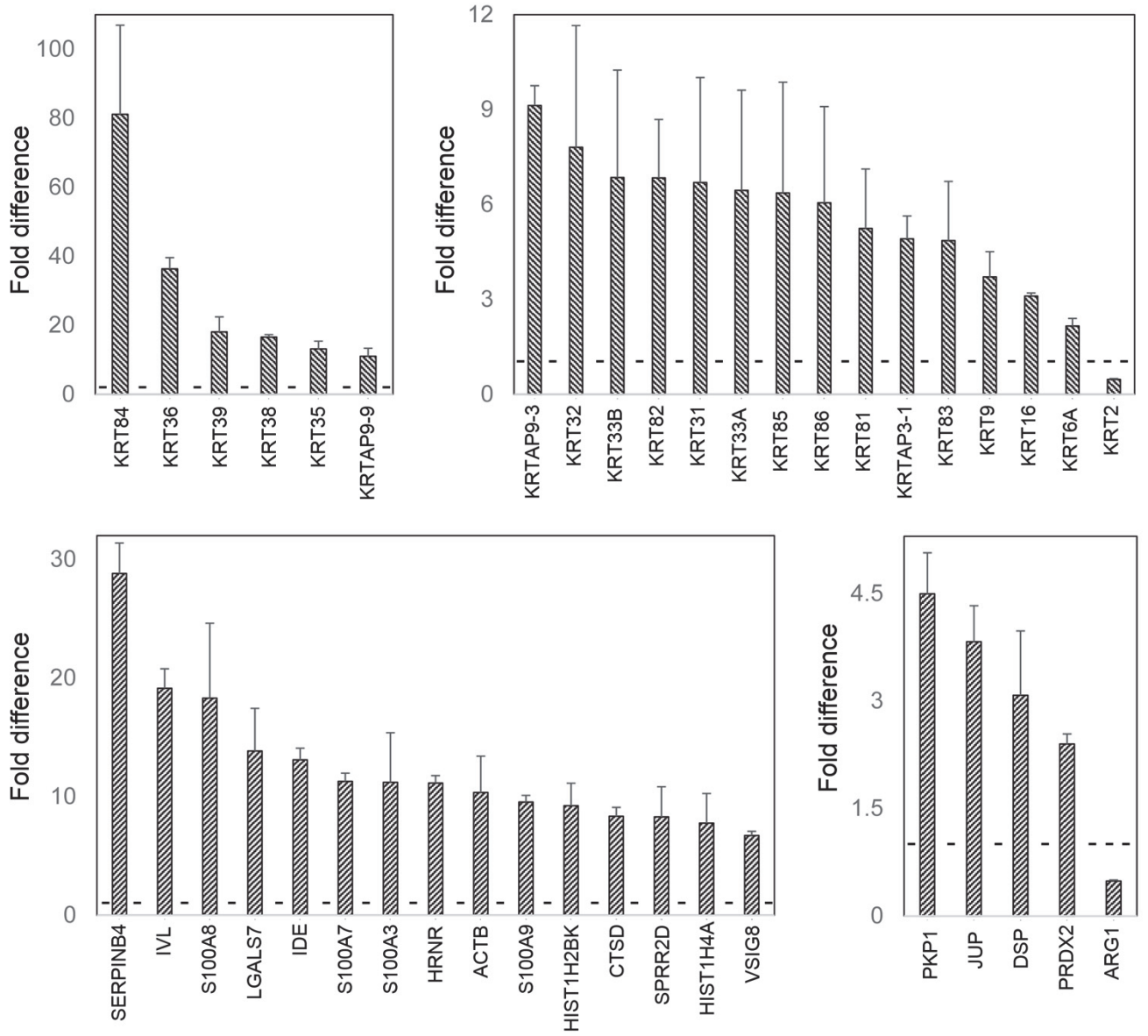

Figure S1. Ratios of protein levels in control samples from forehead to those from leg and arm. Illustrated are those with ratios of weighted spectral counts with at least a two fold difference in forehead compared to arm and leg (averaged with error bars showing the range for arm and leg). The dashed line indicates a ratio of 1. Each protein had >20 spectral counts in forehead samples.

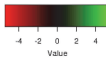

Figure S2. Heatmap showing all the proteins altered in the disease groups arranged in alphabetical order. The map was generated using the Expression tool of Heatmapper software (Babicki S et al [2016] Nucleic Acid Res 44:147-153). Red color indicates down-regulation, while green indicates up-regulation of protein in the samples. Intensities of the colors are proportional to the degree of up or down regulation.

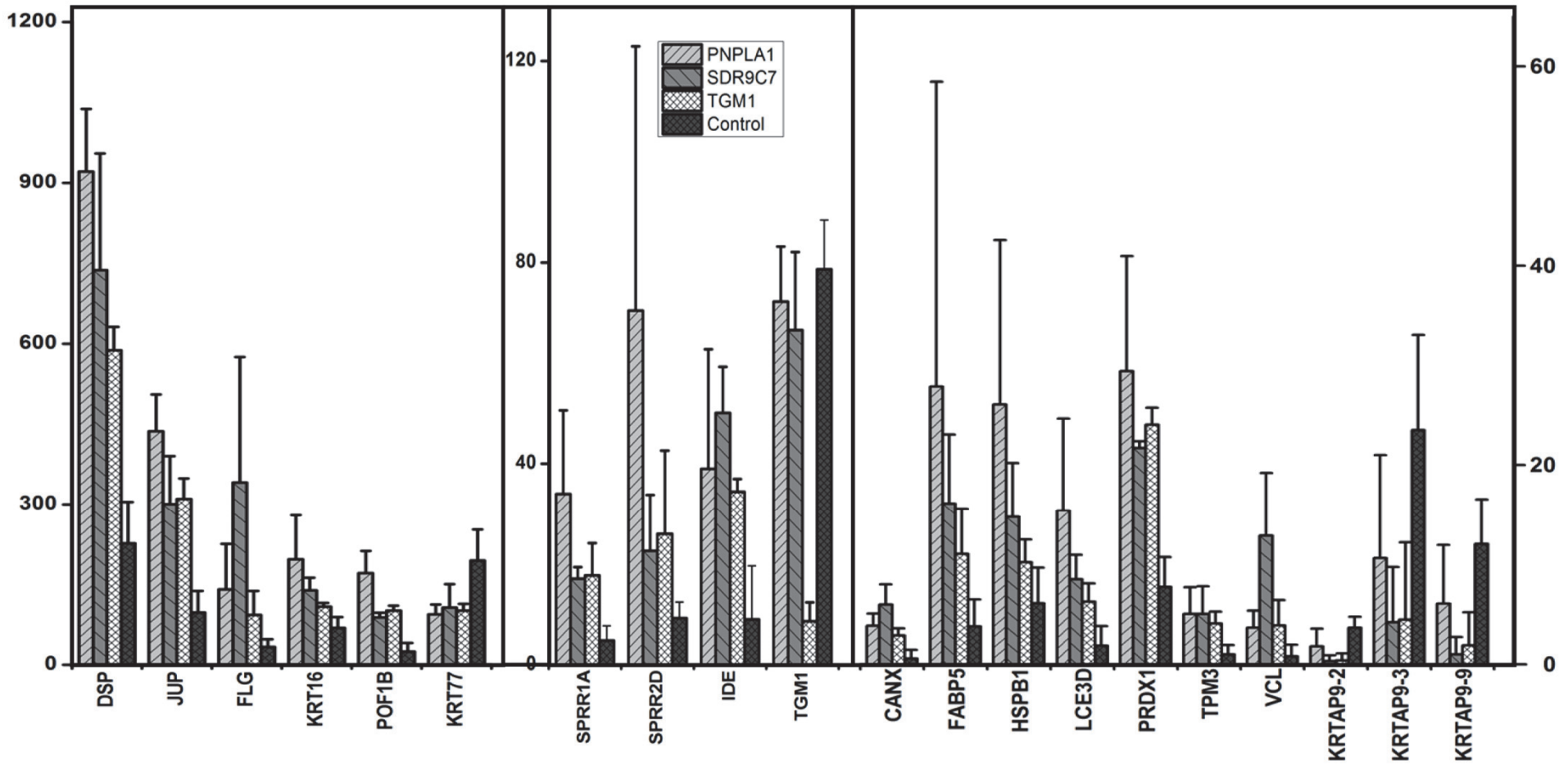

Figure S3: Weighted spectral counts of the 20 proteins common to SDR9C7, PNPLA1, and TGM1 groups.
The error bars represent standard deviations from the mean.

Figure S4. Images of typical scaling patterns.